25th ABCM International Congress of Mechanical Engineering
October 20-25, 2019, Uberlândia, MG, Brazil

COB-2019-0768
CEMENT CURING PROCESS IN THE PRESENCE OF A FLUID LOSS ZONE

Sergio S. Ribeiro
Mônica F. Naccache
Pontifical Catholic University of Rio de Janeiro
225 Marques de São Vicente Street, Gávea - Rio de Janeiro, RJ - Brazil
ssribeiro@gmail.com; naccache@puc-rio.br

Abstract. *This article aims to investigate experimentally and numerically the cementing process of an oil well in presence of filtrate loss zone. An experimental apparatus that physically simulates an oil well annular space was designed and built to investigate the cement curing pressure drop affected by a fluid loss zone. Some experiments were performed with this lab-scale physical well model, and pressure profile could be measured along with the well depth as the cement losses water to the formation. A 2-D transient numerical flow model is proposed and implemented using the finite volume method. Simplified cylindrical Navier-Stokes equations are used to predict pressure, velocity, and cement concentration fields. Cement is modeled as a slightly compressible mixture of two chemical species: a non-Newtonian, thixotropic and pseudo-plastic Bingham gel-like slurry and filtered water. Finally, the simulation results were confronted and contrasted with the experimental data obtained, to validate the numerical model.*

Keywords:*Fluid Loss, Annular Flow, Pressure Drop, Cementing Operation*

1. INTRODUCTION

1.1 Motivation

In the cementing process of oil wells, cement or sometimes resin-based fluids are injected in the annulus to permanently isolate a well zone from the reservoir fluids. The fluid injected must withhold the formation pressures along the well length throughout its curing process. To avoid any fluid exchange until the cement is fully cured, the well relies on the weight of the well fluids.

During cure, the well static pressure suffers a decay, mainly due to a phenomenon called cement shrinkage. It consists of a considerable reduction of the mixture density resultant of the curing chemical reactions. Several authors historically have worked on understanding the pressure decay along the curing process, (Chenevert and Jin (1989);Daccord *et al.* (1991);Prohaska *et al.* (1993);Prohaska *et al.* (1995) and Nishikawa and Wojtanowicz (2002)). On the oil industry, this problem is usually controlled with chemical additives that promote an abrupt increase of viscosity, adjusted to act in the exact moment cement shrinkage occurs. Consequently, precise predictions of pressure drop magnitude and timing are extremely important.

If the formation has highly permeable zones and the well internal pressure is not compatible with the formation pressure, the result is an unbalanced well. Carbonate formations, widely present in the Brazilian pre-salt reservoirs, are known to be very heterogeneous (Tosca and Wright (2015)) and susceptible to partial or total fluid exchanges with the well.

Way before curing begins, uncontrolled fluid loss may also cause a pressure drop in the well. Studies of pressure decay triggered by fluid loss phenomena have been mainly experimental, and most advances made were also in developing chemical additives that would prevent or minimize the filtrate loss itself, as it can be seen on the recent work of Velayati *et al.* (2015)

Computational fluid dynamics is a considerably cheaper initial approach, and can be used to predict the pressure decay along the cementing process, or even indicate where losses might occur in a certain scenario. Therefore, identifying a simple and cost-effective model that provides reasonably accurate predictions is also aimed by this study.

1.2 State-of-art

Generally, due to the huge difference between the characteristic lengths of each dimension in a well, most literature models consider 1-D approximations to describe most flows along the well. However, when analyzing the fluid loss

problem the radial and axial velocities are relevant, and both may vary with radius and length, i.e. $v_r = v_r(r, z)$ and $v_z = v_z(r, z)$.

Chenevert and Jin (1989) elaborated a mathematical model to describe the time evolution of the downhole pressure by calculating a force balance in an annular element. It excludes inertia and considers that a volume reduction of the cement slurry causes a downward movement and consequently a shear force in the opposite direction. Their model also takes into account chemical shrinkage, fluid loss to the formation and gelation by using transient experimental data, but neglects compressibility. The elasticity is considered by employing a simple rheological model to describe the low-shear rate behavior. Later, the mathematical model of Chenevert and Jin (1989) had been solved numerically via finite elements method and the results agree quite well with field data reported by Cooke *et al.* (1983).

Daccord *et al.* (1991) extended their model including mass conservation and compressibility of the slurry. A couple of years later, Prohaska *et al.* (1993) discussed this model in more details, emphasizing the importance of considering pressure effects on gel strength measurements.

More recently, Nishikawa and Wojtanowicz (2002) developed a mathematical expression for predicting the downhole pressure as a function of time based on a dynamic approach. Their 2-D model approximates the annulus by a rectangular slot, neglects inertia and consider a slurry of constant compressibility. Additionally, they assume that chemical shrinkage does not contribute to volumetric change in early stages and that the rheology of the cement slurry is described by the Bingham equation, hence independent of time.

Rodrigues (2019) reviewed thixotropic Cement slurries characterization techniques applied in the literature. In order to characterize cement slurries, they applied modified Herschel-Buckley to fit rheometry measurements of cement slurries and its time-dependent behavior. Finally, Marchesini *et al.* (2019) reviewed widely the past cement slurry curing models, and proposed a thixotropic model based on micro-structure construction and destruction parameters.

1.3 Objectives

The objective of this study is to investigate the cementing process in the presence of a fluid loss zone. This is achieved through simulation analysis and laboratory experimental validation. A 2-D mathematical model is proposed, focused on understanding and predicting the flow on the early curing stages when a highly permeable formation zone produces a radial outflow from the annular.

The scope of this analysis is before the cure chemical shrinkage plays a major role on the pressure decay. At this point, cement column weight is still high, but the mixture viscosity is yet not high enough to prevent water from filtrating into fluid loss zone.

2. METHODOLOGY

All cementing operations are divided in three main phases: mixing, placement and set. As mentioned, the focus is the after placement stage, but before curing shrinkage effects take place. That assumption simplifies the equations so that the inner pipe is assumed static with respect to the formation and the azimuthal velocities can be neglected. Therefore, the model describes a two-dimensional flow, where only the axial and radial directions, z and r respectively, are evaluated.

The overall problem is modeled as an annular flow of a slightly compressible and non-Newtonian fluid, submitted to a filtrate loss zone, as illustrated in Fig. 1. In the schematics, the infinitesimal control volume is represented together with the problem boundary conditions. Here $\vec{g}$ is the gravity acceleration; R_i and R_o are respectively the inner and outer annular radius; and ρ_1 and ρ_2 are the densities of each chemical specie.

As it can also be seen in Fig. 1, the cement mixture is modeled as a mixture composed by two chemical species of densities ρ_1 and ρ_2, but only one specie is filtered into the formation in the fluid loss zone.

2.1 Model Hypothesis and Equations

Although the scope of this study is the after placement flow, it is a transient problem. The chemical reactions considerably change the properties of the fluids, such as viscosity and density, as several experimental works have proven. And despite temperature conditions also influence those properties, with the purpose of this analysis the well is considered isothermal.

As mentioned before, the model considers cement as a single-phase mixture composed by two chemical species, and that only one of those species flows into the formation. That is important to represent local changes on the concentration of each species and consequently capture local mixture density changes, according to Eq. (1).

$$\rho\left(r, z, t\right) = C_1\rho_1 + C_2\rho_2 \tag{1}$$

where r is the radial position; z is the axial position; t is the time; C_1 and C_2 are the concentrations of both chemical species and $C_1 + C_2 = 1$.

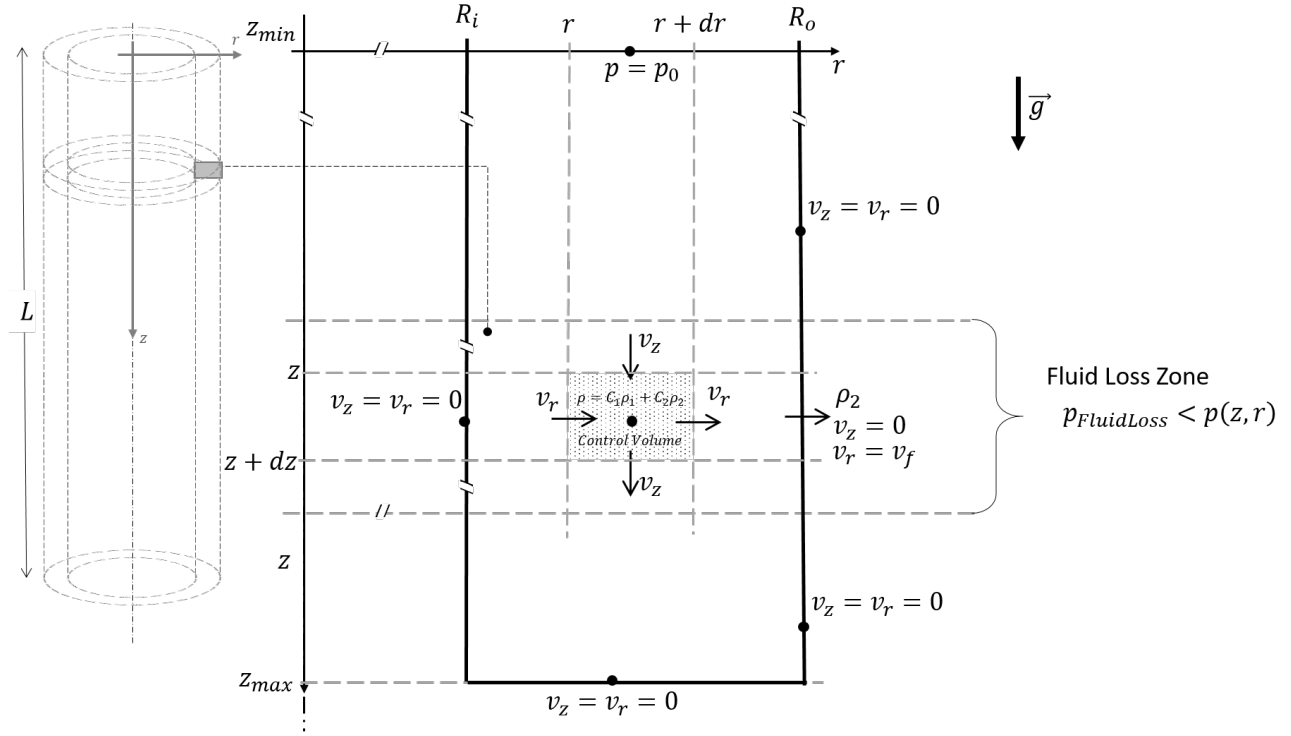

Figure 1. Detailed model schematic with infinitesimal element velocities and boundary conditions represented

Analogously, the mixture viscosity, η, is also calculated from the concentration of each species in a certain control volume. However, the fluid collected from fluid loss experiments, in this case, species 2, is essentially water, with constant viscosity. Hence, the mixture viscosity is defined for each control volume by Eq. (2).

$$\eta\left(r,z,t\right) = C_1\eta_1\left(t,\dot{\gamma}\right) + C_2\eta_2 \tag{2}$$

where $\eta_1(t,\dot{\gamma})$ is the non-Newtonian viscosity of the cement specie, and depends on the time t and on the shear-rate $\dot{\gamma}$; and η_2 is the constant viscosity of water.

The isothermal compressibility state equation can be combined with the mass balance to correlate the changes of pressure p with the concentration of the species, as shown in Eq. (3).

$$\frac{\partial p}{\partial t} = c^2\left(\rho_1\frac{\partial C_1}{\partial t} + \rho_2\frac{\partial C_2}{\partial t}\right) \tag{3}$$

where c is the velocity of sound propagation in the mixture.

Since the concentrations of the species are interdependent, a codification is used in order to solve only one advected field of concentration C_{Code}, where $C_{Code} = C_1 - C_2$. Using this codification, positive values of this field indicates higher concentrations of, and if the field assumes -1 value, the mixture composition is 100% of species 2.

$$\frac{\partial \rho C_{Code}}{\partial t} + \left(\frac{1}{r}\frac{\partial r\rho C_{Code}v_r}{dr} + \frac{\partial \rho C_{Code}v_z}{dz}\right) = \frac{1}{r}\frac{\partial}{\partial r}\left[rD\frac{\partial C_{Code}}{\partial r}\right] + \frac{\partial}{\partial z}\left[D\frac{\partial C_{Code}}{\partial z}\right] \tag{4}$$

where D is the diffusivity of one specie into the other.

Despite the mixture density ρ may change with time, the flow can be considered incompressible, due to its low Mach number. Therefore, the simplified momentum equations are solved for r and z directions, respectively showed in Eq. (5) and Eq. (6).

$$\frac{\partial \rho v_r}{\partial t} + \left[\frac{\rho v_r}{r}\frac{\partial r v_r}{\partial r} + \rho v_z\frac{\partial v_r}{\partial z}\right] = \left[\frac{1}{r}\frac{\partial}{\partial r}\left(r\eta\frac{\partial v_r}{\partial r}\right) + \frac{\partial}{\partial z}\left(\eta\frac{\partial v_z}{\partial r}\right)\right] + \left[\frac{\partial}{\partial z}\left(\eta\frac{\partial v_z}{\partial r}\right) - \frac{\partial p}{\partial r}\right] \tag{5}$$

$$\frac{\partial \rho v_z}{\partial t} + \left[\frac{\rho v_r}{r}\frac{\partial v_z}{\partial r} + \rho v_z\frac{\partial v_z}{\partial z}\right] = \left[\frac{1}{r}\frac{\partial}{\partial r}\left(r\eta\frac{\partial v_z}{\partial r}\right) + \frac{\partial}{\partial z}\left(\eta\frac{\partial v_z}{\partial z}\right)\right] + \left[\frac{1}{r}\frac{\partial}{\partial r}\left(r\eta\frac{\partial v_r}{\partial z}\right) + \rho g_z - \frac{\partial p}{\partial z}\right] \tag{6}$$

Besides, no-slip and impermeability boundary conditions are assumed at the inner and outer walls, except at the fluid loss zone, as detailed previously in Fig. 1.

2.2 Numerical Implementation

The numerical solution of the governing equations is obtained using the finite volume method. Pressure and velocity fields are obtained for given combinations of rheological parameters. Classical finite element methods apply continuous approximation spaces and use volumetric integrals of the weak form. In opposition, finite volume methods approximate piecewise and solve integrals in each cell, yields to exact conservation statements. The volume integrals are converted to surface integrals and the physics is fully specified in terms of the fluxes in those surface integrals.

Regarding the mesh topology, in this work a rectangular mesh is established applying the principle of defining the cell dimensions for each part of the domain and placing the grid points on its center. In order to minimize numerical anomalous results, a staggered mesh ((Harlow and Welch, 1965)) was implemented, as illustrated in Fig. 2.

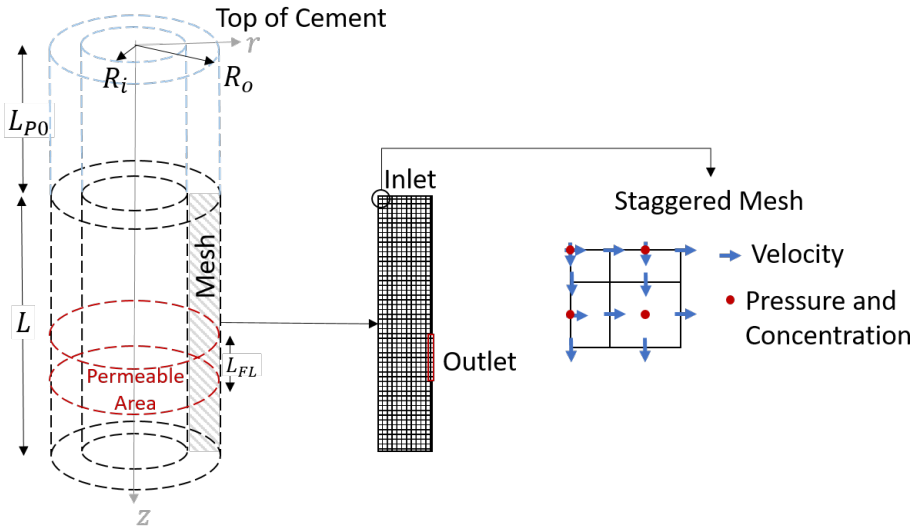

Figure 2. Detailed schematic with mesh domain and where each variable is calculated.

As mass flows into the formation through the permeable zone, the top of cement moves down. The model takes that into account, but without introducing the numerical problems of implementing a free surface boundary condition. As it can be seen in Fig. 2, the inlet boundary is at a depth z beneath the top of cement. Hence, the inlet pressure condition varies with time-based on the weight of the remaining column of cement above(blue dashed line).

Since this is a non-linear problem, pressure and velocities are decoupled and the flow field is solved using a Semi-Implicit method (Patankar and Spalding (1972)), where velocities are calculated with a guessed pressure field, and then both pressure and velocity corrected iteratively based on the mass conservation statement. The spatial discretization scheme used is the Monotonic Upwind for Scalar Conservational Laws, also called MUSCL. The transient simulation workflow is described in Fig. 3.

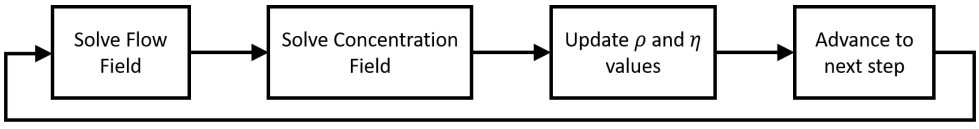

Figure 3. Time iteration workflow.

2.3 Rheological Model

As mentioned before, the non-Newtonian species viscosity depends not only on the shear rate but with time. Hence, the SMD model, presented by Mendes and Dutra (2004), is used to describe the flow curve of a gel-like material where the shear stress τ is a function of the shear rate $\dot{\gamma}$. Using the same methodology presented by Rodrigues (2019), to represent the cement curing the yield stress σ_0 varies with time. Therefore, the cement species viscosity η_{Cem} is defined by the Eq. (7).

$$\eta_{Cem}\left(\dot{\gamma},t\right)=\left[1-e^{\left(-\frac{\eta_0\dot{\gamma}}{\sigma_0(t)}\right)}\right]\left(\frac{\sigma_0\left(t\right)}{\dot{\gamma}}+K\dot{\gamma}^{n-1}\right)+\eta_\infty \tag{7}$$

where $\sigma_0(t)$ is the time-dependent yield stress; K is the consistency index; n is the power-law index and η_∞ is the equilibrium viscosity, estimated as the viscosity at low shear rates; η_0 is the Newtonian level, estimated as the viscosity at very

high shear rates.

3. VERIFICATION AND MESH TEST

Some verification tests were performed, using steady-state Poiseuille flow and transient simple chemical species diffusion as model validation. This verified the model against analytical well-known solutions.

A mesh test was performed and the velocity profile at the annular space was obtained for different sizes of meshes. Figure 4 shows that above around 4000 elements the results converge.

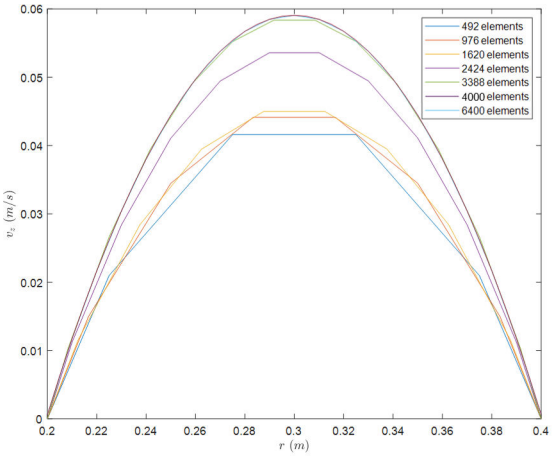

Figure 4. Mesh test performed

4. EXPERIMENTAL SETUP

A large scale lab experiment is used for model validation, with an annular column of cement of eight meters high. This apparatus is fully instrumented for measuring pressure and temperature along its length, as it is shown on the experiments schematics and picture of the installation in Fig. 5.

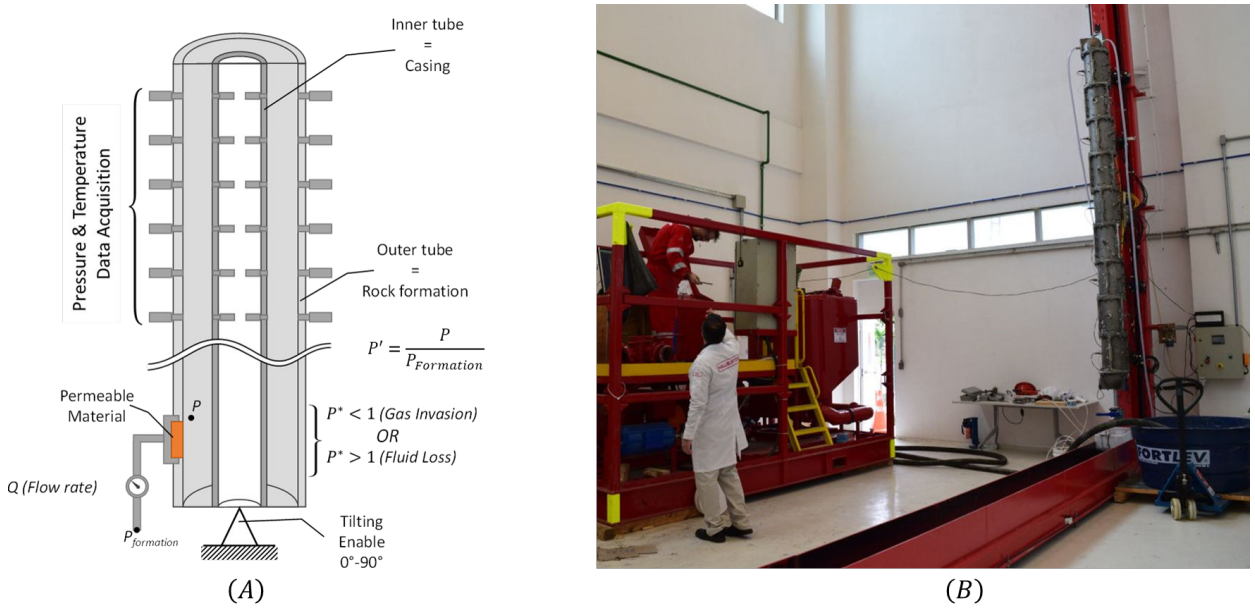

Figure 5. (A) Detailed physical model schematic. (B) Picture of the experimental setup

In Fig. 5, P is the pressure inside the well physical simulator at fluid loss zone height, $P_{Formation}$ is the controlled pressure at the fluid loss zone outlet and P' is the pressure ratio. This well physical simulator is fully configurable and it can simulate formation fluid influx as well as fluid loss. In this study, only one pressure configuration is used for the simulation validation and it is set for the fluid loss scenario.

Other types of equipment were necessary to perform the experiments, such as the cement mixer, as shown on the left

side of the apparatus pictured in Fig. 5. This mixer is an adapted version of an oilfield Batch Mixer, commonly used in field operations of well cementing.

The cement slurry was prepared, pumped in the mold and left curing in the presence of a fluid loss zone with controlled pressure gradient. The water flow rate and the column pressure along the length of the mold were measured during this experiment. This also enabled the calculation of top of cement evolution with time. The results of some tests at this physical Simulator are presented and contrasted with the numerical simulations on the next section.

5. RESULTS

The realized experiments were performed in a partnership between Petrobras and Halliburton, at the Halliburton Technology Center. All simulation results showed correspond to the same experiment performed, and all the parameters used can be seen in Table 1.

Table 1. Case parameters used in the experiment and simulations.

Parameter	Description	Value
L	Simulated cement column height	$2m$
L_{p0}	Initial above cement column height	$6m$
L_{FL}	Fluid loss zone height	$0.1m$
R_o	External annular radius	$1.2m$
R_i	Internal annular radius	$1m$
ρ	Mixture Density	$1200kg/m^3$
μ_{H_2O}	Water(filtrate) Viscosity	$0,001\ Pa.s$
η_{inf}	equilibrium viscosity	$0,295\ Pa.s$
K	Consistency Index	$1.43\ Pa.s^n$
σ_{0D}	Dynamic Yield Stress	$19.19\ Pa^n$
η_0	Newtonian viscosity level	$0.01\ Pa.s$
n	Power Index	0.572

Figure 6 shows the mass of fluid loss collected at the permeable zone with time, and flowrate calculated for each point in time. This flow rate is then fitted and the obtained curve expression is used to calculate the outlet velocity boundary condition.

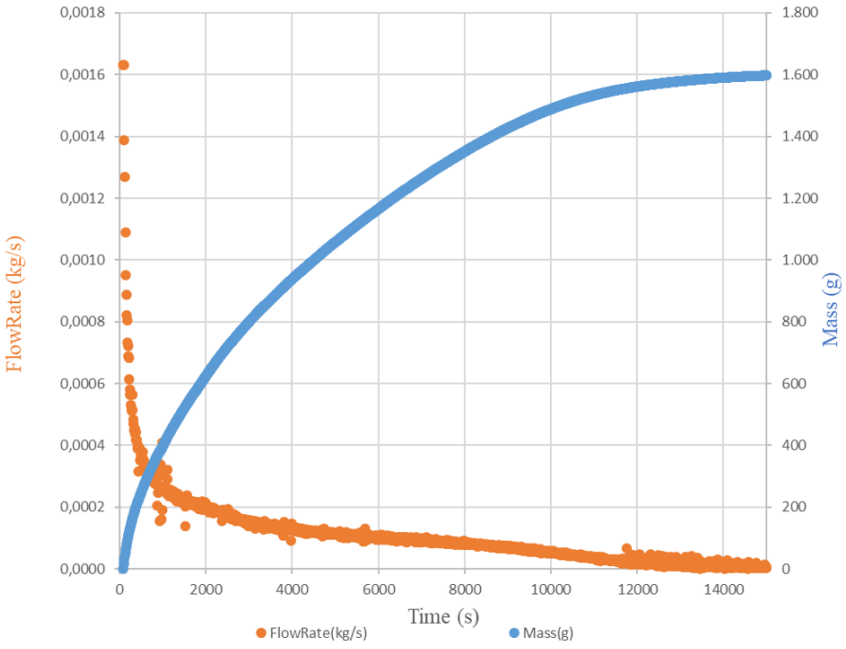

Figure 6. Mass and flow rate evolution with time

In addition, the experimental pressure was recorded through time for discrete points along with the cement column height every $0.4m$. The pressure profiles are plotted for several points in time to evidence the cure pressure drop observed

by the existing literature.

As seen in Fig. 7, the pressure drop observed is accentuated due to the Cement shrinkage, impossible to be isolated experimentally. On the other hand, in Fig. 8 the pressure decay is much smaller for the experimental flow rate of this test. However, the qualitative behavior is similar.

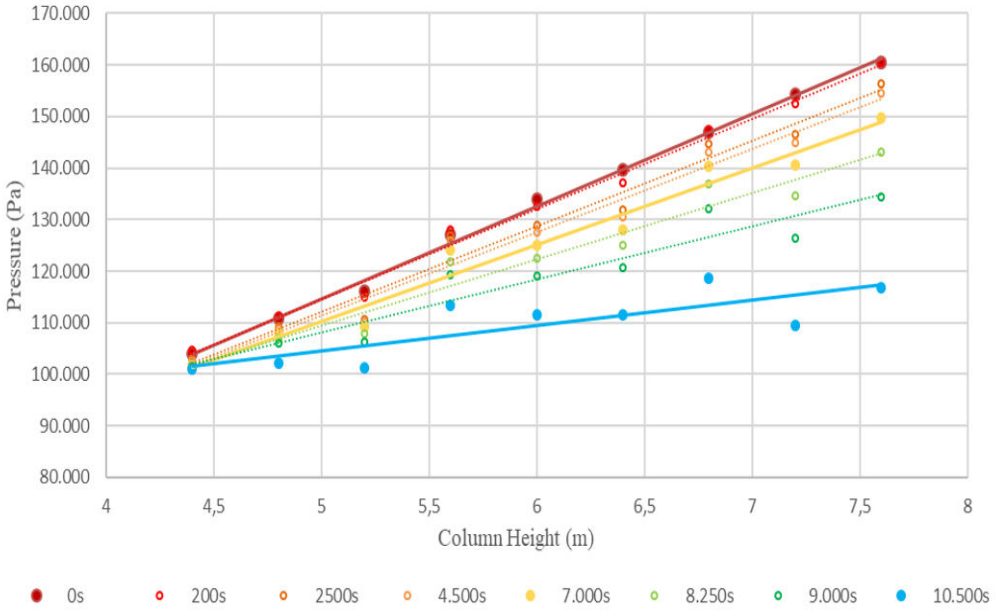

Figure 7. Experimental depth pressure profile evolution with time.

As mentioned, the scope of this study regards evaluating fluid loss and its the pre-shrinkage contribution to the pressure drop. A pressure decay triggered earlier by the fluid loss scenario, may cause more trouble due to low mixture viscosity within the first 40 minutes of cure.

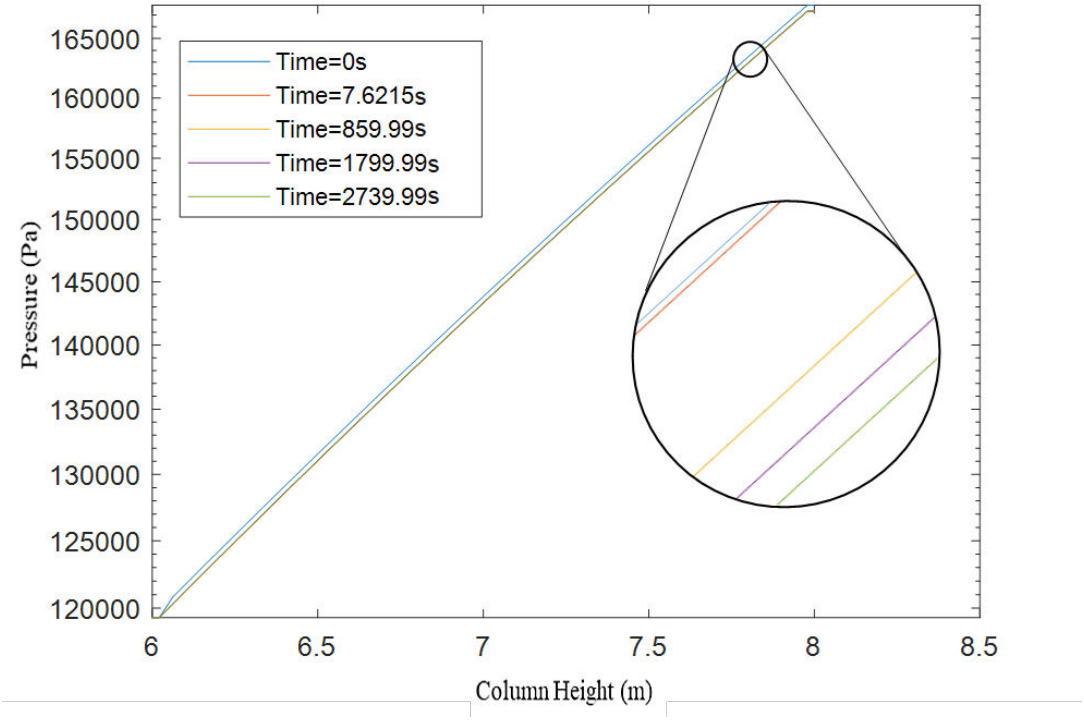

Figure 8. Simulated depth pressure profile evolution with time.

Other aspects also indicate that the qualitative behavior is represented by the model. For instance, at the outlet only one specie is filtered into the rock formation. So, the expected behavior for the cement concentration is to increase with

time close to the fluid loss zone, and propagate inwards according to the calculated diffusion and velocity field. In Fig. 9 and it is possible to see the evolution with time of the simulated scalar field of concentration.

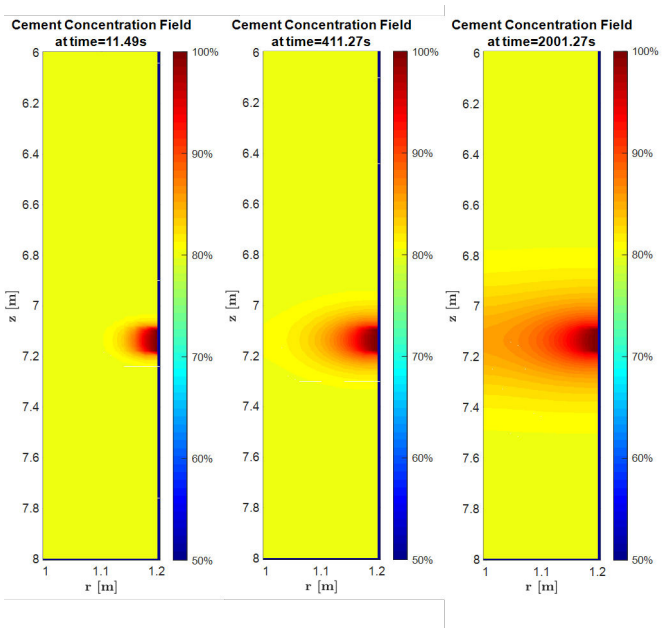

Figure 9. Simulated concentration field evolution with time.

The higher concentrations of cement, directly in contact with the fluid loss zone, are well known by the literature. This extremely viscous layer of cement, it is formed when filtrate loss occurs. This phenomena is observed experimentally not only on wells, but also on press filters cells, and it is called filter cake. It plays a major role on stagnating the well leak with time.

In Fig. 10 velocity and pressure fields are showed in two different moments in time.

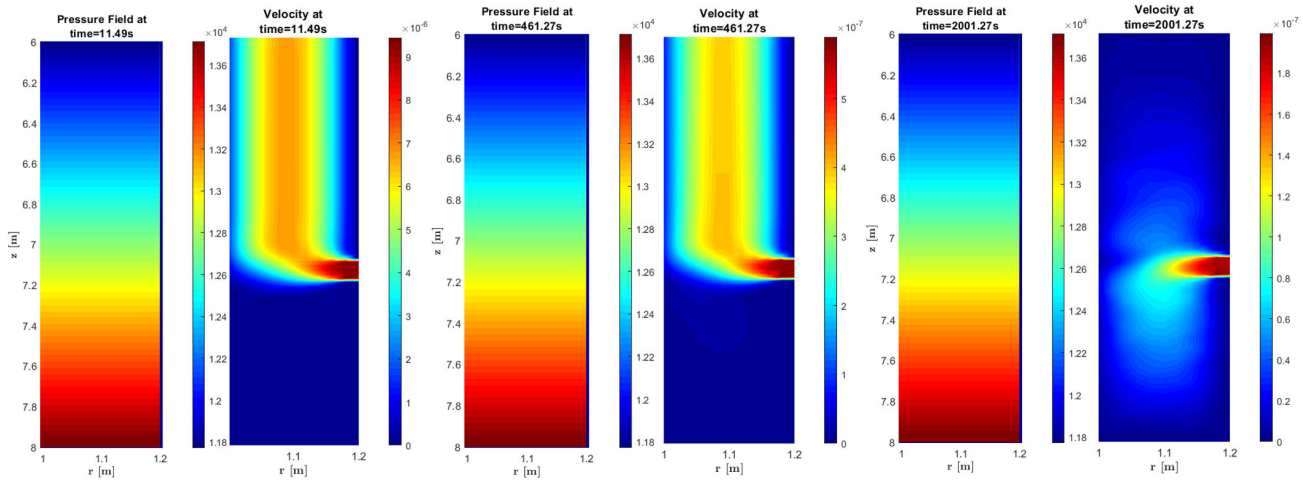

Figure 10. Simulated pressure and velocity fields evolution with time.

At such flow rates, the differences in the pressure profile are hard to detect with this plot. However, the velocity profile changes not only in magnitude but also in form, as seen on Fig. 11. This indicates an increase in the mixture viscosity, also to as predicted.

6. CONCLUSIONS

In this study the cement curing process on oil wells is analyzed in the presence of a filtrate loss zone. A 2D finite volumes model was implemented. A physical simulator was assembled, and used as experimental validation.

Accordingly with the model scope and limitations, the results presented qualitative adherence with the experiment. Pressure profile presented a decay with time as expected. Velocity profile changes evidences the increase of viscosity due

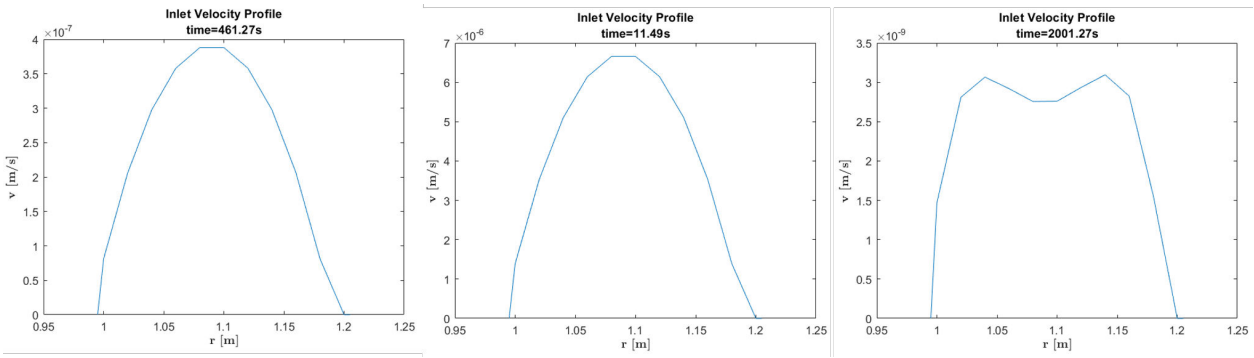

Figure 11. Simulated inlet velocity profile evolution with time.

to lower shear rates.

Concentration of cement field have presented a build-up close to the fluid loss zone. This was also an expected and consistent with the literature description of a filter cake formation.

6.1 Next Steps

To obtain full quantitative adherence, the model will be upgraded with chemical shrinkage support, which relies on the implementation of a mixture density function variable with time.

6.2 Acknowledgments

The authors are indebted to Petrobras, CNPq, CAPES, FAPERJ and Halliburton Energy Services for finantial support, to the Group of Rheology at PUC-Rio. Petrobras and Halliburton also provided the cement slurries and technical guidance to perform the tests.

7. REFERENCES

Chenevert, M. and Jin, L., 1989. "Society of petroleum engineers spe annual technical conference and exhibition - san antonio, texas (1989-10-08) - spe annual technical conference and exhibition - model for predicting wellbore pressures in cement columns". doi:10.2118/SPE-19521-MS.

Cooke, C.E., Kluck, M.P. and Medrano, R., 1983. "Field measurements of annular pressure and temperature during primary cementing". *Journal of Petroleum Technology*, Vol. 35. doi:10.2118/11206-PA.

Daccord, G., De Rozieres, L. and Boussouira, B., 1991. "Cement slurry behavior during hydration and consequences for oil-well cementing". *First International Workshop on Hydration and Setting*. doi:10.2118/19522-PA.

Harlow, F.H. and Welch, J.E., 1965. "Numerical calculation of time-dependent viscous incompressible flow of fluid with free surface". *Physics of Fluids*, Vol. 8, p. 2182. ISSN 1070-6631,1089-7666. doi:10.1063/1.1761178.

Marchesini, F.H., Oliveira, R.M., Althoff, H. and de Souza Mendes, P.R., 2019. "Irreversible time-dependent rheological behavior of cement slurries: Constitutive model and experiments". *Journal of Rheology*, Vol. 63, pp. 247–262. ISSN 0148-6055,1520-8516. doi:10.1122/1.5054879.

Mendes, P.R.S. and Dutra, E.S., 2004. "Viscosity function for yield-stress liquids". *Applied Rheology*, Vol. 14, No. 6, pp. 296–302.

Nishikawa, S. and Wojtanowicz, A., 2002. "Society of petroleum engineers spe annual technical conference and exhibition - (2002.09.29-2002.10.2) - proceedings of spe annual technical conference and exhibition - transient pressure unloading - a model of hydrostatic pressure loss in wells after cement placement". doi:10.2523/77754-ms.

Patankar, S. and Spalding, D., 1972. "A calculation procedure for heat, mass and momentum transfer in three-dimensional parabolic flows". *International Journal of Heat and Mass Transfer*, Vol. 15, pp. 1787–1806. ISSN 0017-9310. doi:10.1016/0017-9310(72)90054-3.

Prohaska, M., Fruhwirth, R. and Economides, M.J., 1995. "Modeling early-time gas migration through cement slurries (includes associated papers 36370 and 36766 and 37387 and 37684)". *SPE Drilling & Completion*, Vol. 10. doi:10.2118/27878-pa.

Prohaska, M., Ogbe, D. and Economides, M., 1993. "[society of petroleum engineers spe western regional meeting - anchorage, alaska (1993-05-26)] spe western regional meeting - determining wellbore pressures in cement slurry columns". doi:10.2118/26070-MS.

Rodrigues, Elias C.; de Souza Mendes, P.R., 2019. "Predicting the time-dependent irreversible rheological behavior of oil well cement slurries". *Journal of Petroleum Science and Engineering*, p. S0920410519303110. ISSN 0920-4105.

doi:10.1016/j.petrol.2019.03.073.

Tosca, N.J. and Wright, V.P., 2015. "Diagenetic pathways linked to labile mg-clays in lacustrine carbonate reservoirs: a model for the origin of secondary porosity in the cretaceous pre-salt barra velha formation, offshore brazil". *Geological Society London Special Publications*. doi:10.1144/SP435.1.

Velayati, A., Kazemzadeh, E., Soltanian, H. and Tokhmechi, B., 2015. "Gas migration through cement slurries analysis: A comparative laboratory study". *Int. J. Min. & Geo-Eng.*, Vol. 49.

8. RESPONSIBILITY NOTICE

The authors are the only responsible for the printed material included in this paper.